Liquid Distribution and Hold-up Measurement in Counter Current Flow Packed Column by Electrical Capacitance Tomography

Liquid Distribution and Hold-up Measurement in Counter Current Flow Packed Column by Electrical Capacitance Tomography

Hao Wu, Bill Buschle, Yunjie Yang, Chao Tan, Feng Dong, Jiabin Jia, Mathieu Lucquiaud

PII: S1385-8947(18)31249-X
DOI: https://doi.org/10.1016/j.cej.2018.07.016
Reference: CEJ 19414

To appear in: *Chemical Engineering Journal*

Received Date: 12 February 2018
Revised Date: 7 June 2018
Accepted Date: 2 July 2018

Please cite this article as: H. Wu, B. Buschle, Y. Yang, C. Tan, F. Dong, J. Jia, M. Lucquiaud, Liquid Distribution and Hold-up Measurement in Counter Current Flow Packed Column by Electrical Capacitance Tomography, *Chemical Engineering Journal* (2018), doi: https://doi.org/10.1016/j.cej.2018.07.016

Liquid Distribution and Hold-up Measurement in Counter Current Flow Packed Column by Electrical Capacitance Tomography

Hao Wu[1,2], Bill Buschle[1], Yunjie Yang[1], Chao Tan[2], Feng Dong[2], Jiabin Jia[1]*, and Mathieu Lucquiaud[1]

1. School of Engineering, University of Edinburgh, Edinburgh, United Kingdom

2. School of Electrical and Information Engineering, Tianjin University, Tianjin, China

Email: Jiabin.Jia@ed.ac.uk

Abstract: In order to meet the requirements and well suit for in-situ process measurement of industrial scale gas-liquid mass transfer applications, such as natural gas processing and post-combustion carbon capture, electrical capacitance tomography (ECT) is used to analyse the distribution of a liquid phase across the packing of a counter current gas-liquid packed column and to quantify the liquid hold-up. The new method eliminates the requirement of a fully flooded reference calibration and only requires vacant and dry calibration steps. The calculation procedure is simplified by using a normal sensitivity matrix which does not include the packing information. The validity of the proposed method was confirmed through finite element method (FEM) analysis studies to certificate neither packing geometry nor orientation relative to the tomography probe nor had a significant impact on phase identification. An experiment is conducted on a counter current gas-liquid packed bed column with 190mm diameter and polypropylene Sulzer Mellapak 250 Y as the packing. According to the experiment with various liquid load, the inclination angle of

structured packing corrugation sheets has an impact on the radial distribution of liquid hold-up in the upper portions of packed beds and liquid hold-up fluctuations of ~0.5% are observable below the flooding limit and even at no gas flow conditions which can meet the empirical correlations from literature. The experiment results show that the proposed method provides the confidence to use ECT in the industrial field service in gas-liquid packed column to provide the real-time liquid distribution and local liquid hold-up measurement.

Keywords: Liquid Hold-up; Liquid Distribution; Electrical Capacitance Tomography; Packed Column; Calculation Model

1. Introduction

Structured packings are tower internals that are used in separation processes such as absorption, distillation, and liquid-liquid extraction. The combination of large surface areas, low gas pressure drops and high separation efficiencies make structured packing ideal for large scale atmospheric gas absorption processes, such as amine based post-combustion CO_2 capture. The effective design and process optimization of these industrial scale absorption towers is strongly linked with the liquid dispersion and gas/liquid interactions within the packed bed.

Structured packing liquid hold-up quantification has traditionally been measured on a packing volume averaged basis through the drain and collect method [1-3]. The

advent of radiation based densitometry allowed for the in-situ quantification of liquid hold-up in structured packing, which enabled liquid hold-up to be calculated at cross sections along the height of the column [4] and provided further information about the distribution of liquid along the height of the packing. This knowledge led to observations that liquid hold-up profiles were unevenly distributed near the interfaces of packing elements and resulted in an evolution in packing element design which featured geometries that smoothed flow between packing elements (e.g. Koch-Glitsch Flexipac-HC, Montz type M, Sulzer MellapakPlus) [5].

Radiation based tomography imaging techniques provided another step change in liquid distribution quantification in packed columns. These techniques are able to characterize and quantify liquid distribution patterns not only along the height of the column but also in the cross section providing critical knowledge on not only liquid hold-up [6] but also 2-D and 3-D hydrodynamic liquid spreading patterns of distillation columns [7; 8], trickle bed reactors [9] and counter-current gas-liquid columns with structured packing [10]. Recently Jenzen [11; 12] used ultra-fast x-ray tomography to demonstrate a step change in tomographic techniques for packed bed hydrodynamics that enabled observation of dynamic liquid load and liquid distribution on timescales that were relevant to the hydrodynamics of the system (temporal resolution of 2000 frames per second and spatial resolution of 1 mm). Dual-plane x-ray tomography has also been used to determine phase fractions and local velocity distributions in a fluidized bed application [13].

Experimental hydrodynamic data extracted from these tomography systems can

be used to validate the complex mathematical modelling efforts of liquid distribution over tower internals with complex geometries and can supplement traditional experimental campaigns leading to a richer understanding of modelling mass transfer systems. Mechanistic liquid distribution models [14], two phase immiscible flow models [15], and computation fluid dynamics (CFD) simulations [16] used in modern mass transfer modelling could all benefit from enhanced hydrodynamic knowledge of real systems.

While ultra-fast x-ray tomography is able to provide critical information on industrially relevant metallic structured packings at the lab scale, the inherent nature of high energy radiation measurements means the costs of instrument systems and practicalities of safely handling the radiation are impractical for industrial based field measurements. In contrast, electrical measurements have been used as an alternative to radiation based densitometry for in-situ quantification of liquid hold-up in structured packed beds. Both electrical capacitance [17] and electrical resistance measurements [18] have been demonstrated to produce liquid hold-up measurement accuracies similar to radiation based techniques while also having the benefit of drastically reduced costs, orders of magnitude higher acquisition rates, and safer installation and use. It has been suggested that electrical measurements may be scalable and appropriate for industrial field service [17].

Tomography systems based on electrical measurements has been deployed in various industrial field service applications to characterize and quantify two-phase fluid flows both with and without fixed structural internals. Electrical Resistance

Tomography (ERT) systems have been used to investigate the mixing characteristics in a packed-bed external loop airlift bioreactor [19], the effect of particles and liquid load on the phase distribution in trickle bed reactor [20], and gas distribution and void fraction in a packed bubble column with different packing materials [21]. Son et al. used ERT to measure the liquid distribution in pilot-scale packed column, in order to study the effects of the liquid load, gas factor, and liquid properties on the liquid distribution under various offshore conditions [22]. Similarly, Electrical Capacitance Tomography (ECT) systems have been used to investigate pulse flow and pulse velocity in co-current trickle bed reactors [23] and solid phase distributions in a gas-solid fluidized bed [24]. Hamidipour used a twin-plane ECT to study the hydrodynamics of gas-liquid co-current down-flow and up-flow packed beds by cross-correlating each plane's tomogram to axial dispersion residence time distribution and modelled liquid hold-ups and pseudo-interstitial velocities for pulsed flow in the system [25].

Operators of industrial scale mass transfer operations that are highly dynamic in nature, such as post combustion CO_2 capture systems with varying gas inlet flows and varying product recovery constraints, would benefit from real time in situ hydrodynamic data of the column internals. This information could be used to reduce settling time between plant states, increase process agility, troubleshoot reactors that are operating outside of design specifications, and allow for more efficient operation at off-design conditions.

When considering the development of this type of measurement system, several

practical considerations make electrical capacitance tomography (ECT) a strong choice for the measurement technology. Absorption mass transfer operations (e.g. aqueous amine based post combustion CO_2 capture) are gas phase dominant, therefore electrical capacitance measurements preferred over conductivity measurements which would prefer a continuous liquid film path between each sensor array contact. The in-situ process probes would be low cost to manufacture, safe to operate, free of moving parts, and could be coated to increase corrosion resistance as they would not be required to directly contact the fluid or packing. Obvious drawbacks remain: in-situ tomography is unable to extract data that is critical for the effective modelling of mass transfer reactions such as local velocity distributions, fluid composition measurements, and film and rivulet liquid parameters necessary to quantify the true liquid surface area. Further electrical capacitance tomography will struggle to image systems that utilize a grounded metallic packing phase, which is the current industry standard for many mass transfer applications. The coating of metallic packing by the nonconductive material will improve the performance of the ECT measurement.

Nevertheless, the potential merits of an ECT instrument system that is fit for industrial scale applications warrant further investigation. This work develops a measurement technique appropriate for industrial applications, evaluates the technique's robustness and measurement accuracy through a FEM approach, and compares the measurements of a prototype ECT instrument system against traditional lab based quantification techniques in a counter current gas-liquid column fitted with polypropylene Mellapak 250.Y structured packing.

In developing an ECT measurement system that is fit for industrial field service, the practicalities of field calibration and operation must be considered. In typical electrical tomography systems, it is difficult to relate the electrical measurement tomogram to physical liquid loadings because the local electrical field is affected by many ancillary factors such as 3-D geometry of the liquid film and the inherent electrical conductivity of the liquid as well as the volume of liquid present. Some compensation method should be used according to the research [22]. In industrial scale operations however, these compensation mechanisms may not be practical. Fully submerging the packed column in the absorption solvent is likely impossible in most scenarios. Further performing local liquid collections and sudden stop and start operations required for the drain and collect method would require significant effort and liquid level measurement difference calculations would have to include complex volumetric compensations for pipe runs, heat exchangers and redistribution equipment.

The alternative demonstrated in this work constructs a tomogram image and determines liquid hold-up from a calculation model with single reference, and uses a normal sensitivity matrix which just includes the pipe wall information (to simplify the calculation procedure) for the liquid hold-up calculation. This methodology has several benefits, namely:

1) Eliminating the need to take a background tomogram with a fully submerged column.

2) Simplifying the calculation to neglect electrical field complexities not related

to liquid hold-up, eliminating the need to regress signals against volumetric hold-up measurements.

3) Simplifying the calculation by using a normal sensitivity matrix calculated by FEM without including the packing information, which can be used for different packing structures, column diameters and liquid conductivities.

4) Allowing FEM to be a useful tool to analyse and quantify the effective measurement error in the application that cannot be validated by the experiment conveniently.

These benefits would enable the measurement system to be practically deployed on existing plant facilities with reasonable installation and commissioning times. Further the designed calculation model for the ECT could realize the online liquid hold-up calculation and liquid distribution reconstruction in the practical packing column application.

2. Liquid Hold-up Calculation Model by ECT

In this work, a liquid calculation model for ECT is designed that does not have to submerge the column to make the calibration. This model can be used to deal with different packing structure and is easy to be used in the field application. In the packed column with the gas, liquid and packing, when the permittivity of liquid is much larger than that of the other two substances, the ECT is able to differentiate liquid to calculate the liquid hold-up and reconstruct the liquid distribution.

2.1 Principle of ECT

ECT measures capacitance between the electrodes, then reconstructs the relative permittivity distribution in the sensitive field. Both forward problem and inverse problem are involved in ECT. For the forward problem, a linearized relationship between the normalized permittivity distribution g and the normalized capacitance data C_{norm} is:

$$C_{norm} = Sg \tag{1}$$

where S is the sensitivity matrix. For the typical inverse problem, the target of ECT reconstruction is to estimate the permittivity distribution based on measured capacitance. The conventional image reconstruction algorithm was reviewed in [26] with spatial resolution of 5% of the column diameter [27].

The measurement principle and structure of ECT system is shown in Fig. 1.

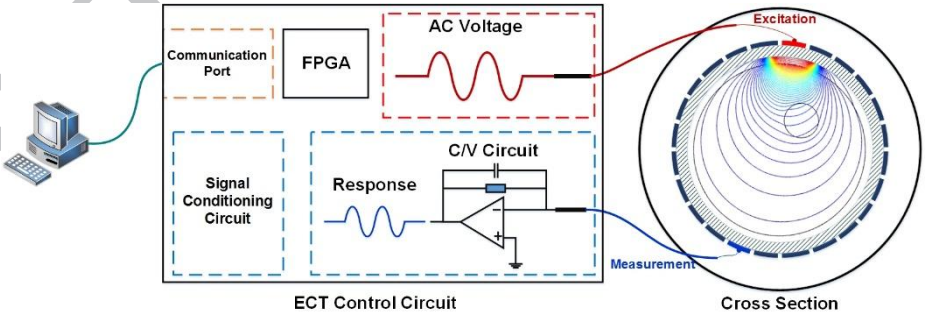

Fig.1. Measurement principle of ECT

The ECT measurement system includes ECT sensor, control circuit and computer. In this application, the ECT sensor is made by copper foil, with measurement

electrodes, guard electrodes and shield electrode. A sine wave voltage with 14 $V_{p\text{-}p}$ and 200 kHz frequency is used as the excitation signal. One measurement electrode is chosen for excitation; other electrodes are used to acquire the signal separately. The acquired signals are conditioned by the C/V circuit and other conditioning circuit, then transmitted to the computer through the USB communication port. The FPGA controls the switching circuit and switches the excitation and measurement electrodes for the next measurement. After the excitation signal traverses all electrodes, it accounts as a frame. The frame rate of the ECT system is 714 frames per second. The maximum signal-noise-ratio (SNR) is 76.73 dB and the minimum SNR is 62.25 dB amongst all the channels [28; 29].

2.2 Liquid Hold-up Calculation Models

In the previous research, the parallel model was used for the stratified two-phase dynamic flow with packing [17]. In terms of different two-phase flow mixture, either parallel model in equation (2) or series model in equation (3) can normalize the measured capacitance [30]:

$$C_{norm} = \frac{C_{mea(j)} - C_{l(j)}}{C_{h(j)} - C_{l(j)}}, \quad j = 1,2,\ldots,P \tag{2}$$

$$C_{norm} = \frac{\dfrac{1}{C_{mea(j)}} - \dfrac{1}{C_{l(j)}}}{\dfrac{1}{C_{h(j)}} - \dfrac{1}{C_{l(j)}}}, \quad j = 1,2,\ldots,P \tag{3}$$

where j is the location of the measurement projection, P is the maximum number of

measurements. $C_{mea(j)}$ is the measured capacitance at the j^{th} location. $C_{l(j)}$ and $C_{h(j)}$ are the reference capacitance at the j^{th} location when the sensitive field is full of low permittivity media and high permittivity media separately.

In industrial field applications, the full calibration with high permittivity media $C_{h(j)}$ is inconvenient to acquire as it would require the column cross section to be flooded with liquid. Therefore, a normalization method with single reference media only is developed in this work in order to expand the ECT's application. The normalization model is expressed in equation (4):

$$C_{norm} = \frac{C_{mea(j)}}{C_{ref(j)}}, \quad j = 1,2,\ldots,P \tag{4}$$

where $C_{ref(j)}$ is the reference capacitance when the packed column is full of low permittivity media, i.e. gas or gas with packing.

Within the ECT sensing field, the permittivity distribution and measured capacitance have an approximately linear relationship:

$$\frac{C_{mea(j)}}{C_{ref(j)}} \approx \frac{\sum_{k=1}^{w} \varepsilon_{mea(k)} s_{j,k} \left(\varepsilon_{mea(k)}\right)}{\sum_{k=1}^{w} \varepsilon_{ref(k)} s_{j,k} \left(\varepsilon_{ref(k)}\right)} \tag{5}$$

where k is the pixel number of the sensitive field and w is the maximum number of pixels. $\varepsilon_{mea(k)}$ and $\varepsilon_{ref(k)}$ are the measured permittivity and reference permittivity at the k^{th} pixel respectively. Sensitivity matrix S is calculated using the FEM. The element of normalized S is $s_{j,k}$, which describes the mapping relationship between the j^{th} measurement projection and the k^{th} pixel on the image. The ratio of $\varepsilon_{mea(k)}$ and $\varepsilon_{ref(k)}$ is derived from equation (5) and shown in equation (6).

$$\frac{\varepsilon_{mea(k)}}{\varepsilon_{ref(k)}} \approx \frac{\sum_{j=1}^{P} \frac{C_{mea(j)}}{C_{ref(j)}} s_{j,k}\left(\varepsilon_{ref(j)}\right)}{\sum_{j=1}^{P} s_{j,k}\left(\varepsilon_{ref(j)}\right)} \tag{6}$$

The Ramu-Rao's model [31] is used to calculate the relationship between phase fraction and the phase permittivity. For two-fluid immiscible two-phase flow, the low permittivity phase is continuous phase, the permittivity of the two-phase mixture depends on the high permittivity phase in mixture ratio (HMR) when the mixture can be assumed as homogeneous flow:

$$\varepsilon_{mixture} = \varepsilon_{low} \frac{1+2HMR}{1-HMR} \tag{7}$$

where $\varepsilon_{mixture}$ is the permittivity of the immiscible two-phase mixture, and ε_{low} is the permittivity of low permittivity phase.

According to the assumption of Ramu-Rao's model, the permittivity of the two phase should have huge difference. In the packed column with gas, liquid and packing three different media, the relative permittivity of liquid (i.e. water is ~80) is much larger than that of packing (i.e. polypropylene is ~2.2) and gas (~1). When these three media in the sensitive field is assumed as homogeneous flow, the liquid in mixture ratio (LMR) can be obtained from the Ramu-Rao's model based on Maxwell equations:

$$LMR \approx \frac{\varepsilon_{mea(k)} - \varepsilon_{ref(k)}}{\varepsilon_{mea(k)} + 2\varepsilon_{ref(k)}} = \frac{\varepsilon_{mea(k)} / \varepsilon_{ref(k)} - 1}{\varepsilon_{mea(k)} / \varepsilon_{ref(k)} + 2} \tag{8}$$

2.3 Liquid Hold-up Calculation Procedure

ECT has been used in many applications for two-phase flow measurement. In the packed column, as three different media with different relative permittivity (gas /packing/liquid) are existed in the sensitive field, it will cause the difficulties for the ECT measurement and data analysis. The sensitivity matrix *S*, which is calculated by the FEM simulation, is a key parameter in the liquid hold-up calculation and distribution reconstruction. The common sensitivity matrix *S* just includes the information of pipe wall, and does not contain the packing information. If it is used directly in the packed column, it will cause a large error of quantitative measurement for liquid hold-up and liquid distribution analysis.

In order to realize the accurate measurement, the sensitivity matrix containing both the gas phase and the fixed packing is required. However, modelling the complex packing geometry in the FEM software is complex. Even after the FEM model computed the accurate sensitivity matrix including the packing information, the orientation of ECT sensor electrodes relative to packing should match the FEM model for the *S* matrix to be valid. This method is complex and almost impractical to be used in the field application.

For the purpose of solving this problem, the alternative proposed here is to use the common sensitive matrix S (only includes the pipe wall information) for the calculation. After the calibration with gas, the real time gas/liquid/packing ECT results are used to subtract the gas/packing results to acquire the liquid hold-up present in the system.

The ECT can be used to compute the packing column with any packing

geometry based on this alternative. It is a fundamental methodology for designing electrical tomography systems from electricity principles rather than calibrating and correlating with liquid hold-up measurements.

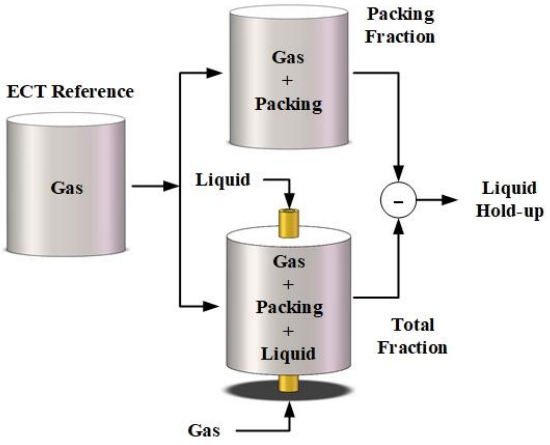

Fig.2. Calculation procedure for ECT measurement in packed column

The detailed procedure is shown in Fig. 2:

Step 1: The column is full of gas at first to take reference, in order to get C_{ref} in equation (4). The common sensitivity matrix S is calculated by the simulation with an empty field (empty column full of gas with relative permittivity of 1).

Step 2: The packing material is added into the packed column. The capacitance of gas/packing mixture is measured by ECT again, to get the C_{mea} with packing. The measured capacitance can be used to calculate the packing fraction.

Step 3: The liquid is sprayed from the top of the column and gas is added from the base of the column, the ECT measures the capacitance of the gas/liquid/packing mixture. The model will be used to calculate the total fraction of packing and liquid.

Step 4: The result in step 3 subtracts the result in step 2 to get the liquid hold-up

in packed column.

3. Calculation Method Validation Through Finite Element Model

In order to validate the calculation method, two FEM modelling investigations were employed. The first investigates the influence of packing geometry on the calculation method by normal sensitivity matrix to determine if different packing shapes and orientations have an effect on the packing fraction calculation in the gas/packing reference tomogram. The second simulates a 190mm experimental test rig fitted with capacitance probe contacts and estimates the liquid hold-up measurement accuracy for Mellapak 250.Y PP under a range of dynamic liquid hold-up.

3.1 Parametric Study of Packing Geometry

Packing can have a variety of geometric structures (e.g. corrugation and inclination angles, perforated sheets and gauze materials) that are customized for different applications. The geometric structure of the packing may have an influence on the capacitance calculation, which could impact the accuracy of the calculation method. FEM simulation is used to calculate the sensitivity matrix, therefore accurately describing the geometric structure in the FEM simulation could be important. However, accurately describing the geometric structure in the FEM simulation is impractical for two reasons. First, the actual geometry of real packing materials is really complex due to manufacturing variations such as sheet and gauze

surfaces inconsistencies, perforation locations, and the existence fasteners and wall wiper bands. Second, the orientation of the ECT sensor electrodes relative to structured packing out in the field is unlikely to match what is represented in FEM simulation.

In order to assess the effect of packing geometry on the calculation method with normal sensitivity matrix a parametric study was performed where packings of various geometric structures but the same volume was simulated in the FEM software as shown in Fig. 3. The internal and external diameter of the pipe were set to 190mm and 200mm respectively within the FEM model, which is identical to the experimental test rig. The FEM model included eight measurement electrodes are located on the outside of the pipe wall with 0.88 duty ratio and a shield electrode located at the outside of the pipe and connected to the ground, which also matches the experimental test rig. The space between the shield electrode and pipe wall is set as air with relative permittivity 1. The packing material is configured as polypropylene with relative permittivity 2.2. A common sensitivity matrix which does not include the information of packing is used in simulation. Each packing geometry and the packing volume were then calculated using the common sensitivity matrix and the calculation method described in section 2.3.

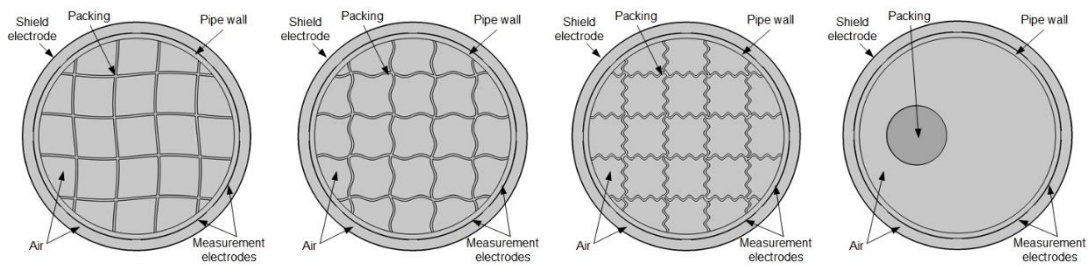

(a) (b) (c) (d)

Fig.3. 2D simulation models with different packing structure

As seen in table 1, the calculation method underestimates the true value of the packing fraction, but the underestimation is similar in magnitude for each packing geometry implying that packing geometry does not have an effect on the packing fraction calculation, this is very important in the liquid hold-up calculation step. (The fraction is considered as a relative quantity, the "absolute error" will be used as the calculation error to evaluate the performance).

As packing geometry does not have an effect on the packing fraction and liquid hold-up calculation, the combination of common sensitivity matrix and calculation method can be used on any type of structured or random packing type where the packing fraction is known. Additionally, this finding would imply that the ECT sensor electrodes could be installed anywhere along the column without considering its orientation relative to the packing, which would be a very convenient feature for industrial field applications.

Tab.1. Calculation results for 2D simulation model

Packing structure	a	b	c	d
Packing area (mm^2)	2596	2596	2601	2596
Packing fraction	9.156%	9.156%	9.173%	9.156%
Calculated packing fraction	7.80%	7.57%	7.88%	7.81%

Calculation error	1.356%	1.586%	1.293%	1.356%

3.2 Evaluation of Measurement Accuracy

Having established that the packing structure does not have a significant influence on the calculation method, FEM analysis is used to assess the robustness and accuracy of the calculation model when measuring fluids of both high and low permittivity. Fig. 4 shows the 3D model of the viewing field as built in the FEM software with dimensions that match the experimental test rig and a structured packing as shown in Fig. 3(b).

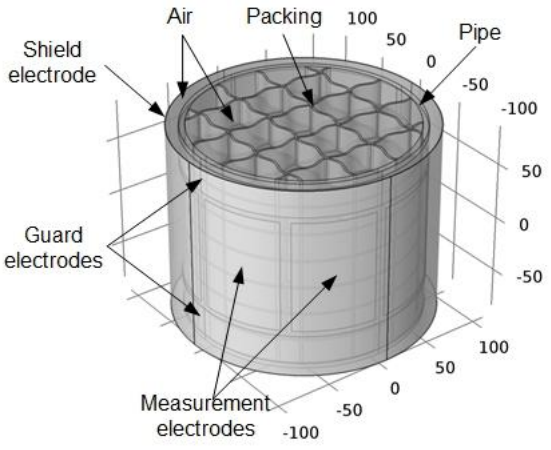

Fig.4. 3D simulation model of packed column for ECT measurement

The internal and external diameter of the pipe is 190mm and 200mm. The height of the pipe is 170mm. The shield electrodes are located at the outside part of the pipe and the guard electrodes are located at the top and bottom part of the pipe with the 25mm height. The height of the eight measurement electrodes is 100mm and duty

ratio is 0.88. The pipe wall material is set as plastic with relative permittivity 2.2 and all the electrodes of ECT are set as copper. The space between the shield electrode and the outside pipe wall is set as air with relative permittivity 1, which is the same as the real ECT sensor. The detailed packing structure is displayed in Fig.5, where many layers are added to simulate the real packing structure and to increase the packing fraction to 13.96%.

Liquid was simulated by adding 774 dispersed liquid droplets with a diameter of 8mm (equivalent to 7.32% of the packed volume) inside each packing cell as shown in Fig. 5. The permittivity of each droplet can be controlled within the FEM software, switching it between liquid and gas to simulate variable levels of liquid load on the packing.

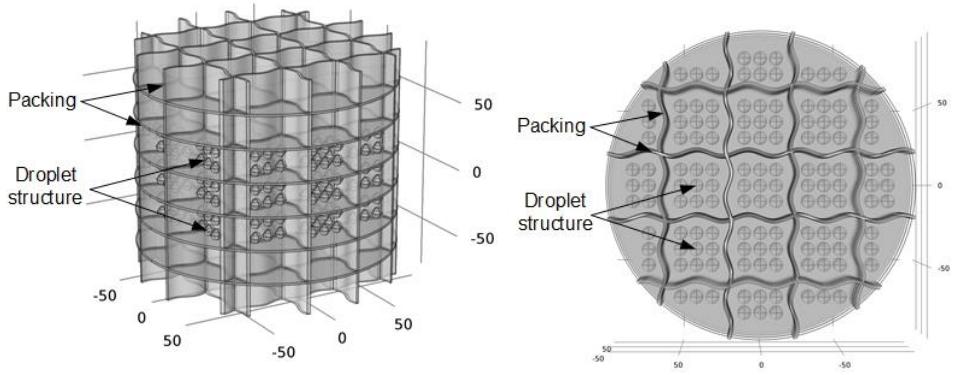

(a) Oblique view (b) Top view

Fig.5. Packing and liquid droplets in simulation

As stated previously, the calculation model is designed to operate without taking a reference measurement of high permittivity media for convenience of industrial

applications. In order to compensate the media fraction measurement results different relative permittivity, a coefficient α is be applied to correct the liquid hold-up F_L, as expressed in equation (9).

$$F_L = \frac{LMR}{\alpha} \tag{9}$$

The correction coefficient α in equation (9) could have two implications of on measurement performance in industrial applications. First, accurate determination of the permittivity of the liquid phase being analyzed could be a non-trivial and important step during instrument calibration and commissioning. Second, process operations that can alter the liquid's permittivity over time (absorption of ions, chemical changes, etc.) may cause an undesirable measurement drift. FEM modelling was used to determine the correction coefficient α for relative permittivity range of 1-100. In this simulation, the relative permittivity of all 774 droplets are set to a value and the liquid hold-up of 7.32% is calculated from equation (8) to find α in equation (9) as shown in Fig. 6.

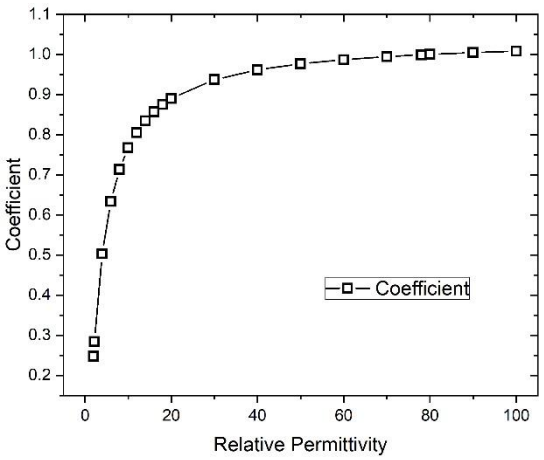

Fig.6. Coefficient α calculation

The FEM simulation shows that the behavior of the coefficient of the model is non-linear in nature. For the solutions with a relative permittivity in the range of 60-100, the fraction calculation results by the model is almost close to the bench mark because the α is equal to ~1. This would imply that for ECT system analyzing aqueous solutions, the single point calculation method proposed in this work would be fairly accurate without the use of a correction factor. For the solutions with a relative permittivity in the range of 1-60, the coefficient α is needed to revise the calculation results to improve the performance. The assumption of the model in section 2.2 that the permittivity of the measured phase should be much larger than that of the other media has also been validated by this non-linear property of coefficient α.

Having established that the relative permittivity of the aqueous absorption liquid would have a negligible impact on liquid hold-up measurement performance, the measurement accuracy of the calculation method was estimated in the FEM software by simulating various levels of liquid hold on the packing material. An appropriate number of the 774 droplets present in the FEM software were randomly selected to represent the stochastic nature of liquid film forming on the packing. Fig 7 shows the liquid hold-up calculated using the method described in section 2 compared with the actual hold-up of liquid droplets present in the FEM simulation.

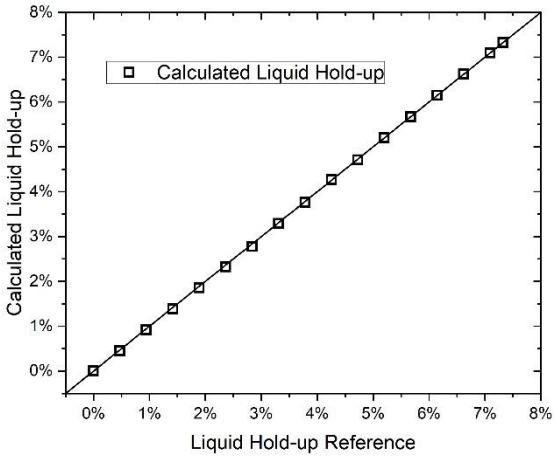

Fig.7. Calculated liquid hold-up

The simulation results show that the measurement method may be consistently accurate over a range of liquid hold-up values from low static hold-up (< 1%) to heavily loaded dynamic hold-up values (> 6%). Utilizing the FEM simulations allows the calculation method to be validated against fundamental electric field equations, confirms that the methodology assumptions and simplifications do not adversely affect the measurement performance for a typical gas-liquid absorption application, and is able to provide confidence that the method and sensor system have potential in an industrial field application.

4. Experimental Description

A packed column test rig was constructed to simulate a small scale gas-liquid absorption application as shown in Fig 8. The internal and external diameters of the column are 190mm and 200mm and the packing consisted of two sections of Mellapak 250.Y PP of 315 mm in height followed by two additional section of 157.5

mm in height. Packing sections are 180 mm in diameter and rotated 90 deg from each other.

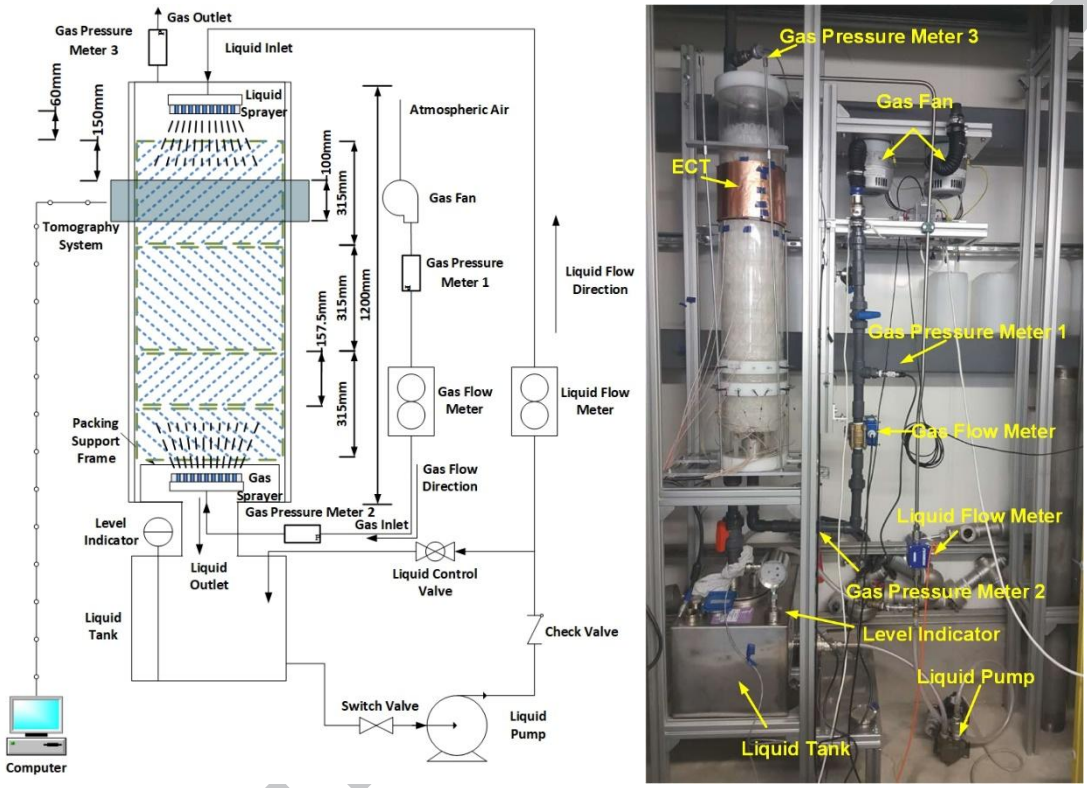

(a) Schematic diagram (b) Photo of experimental flow loop

Fig.8. Pilot scale experimental flow loop

Liquid is pumped from the tank and sprayed through a nozzle located at the top of the column and described in Fig. 9. Liquid flow is controlled with an adjustable bypass valve and monitored with an electromagnetic flow meter (OMEGA, FMG71B-A-BSP, with an accuracy of ±2.0%).

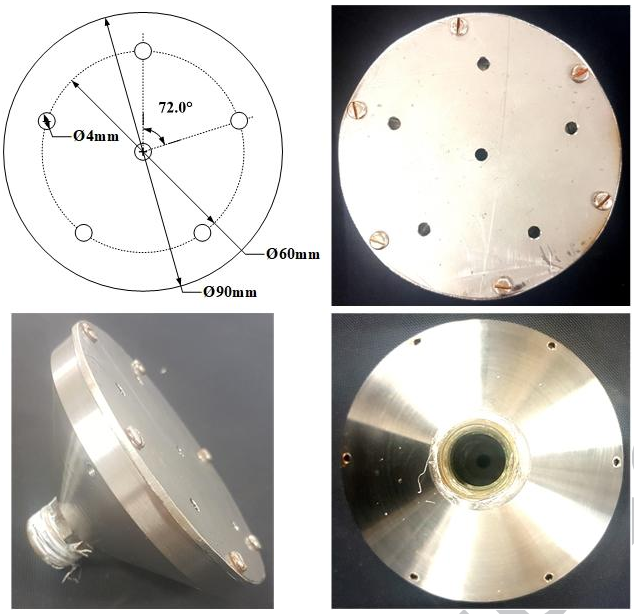

Fig.9. The dimension and the photos of the liquid sprayer.

A high accuracy level indicator (KSR KUEBLER, FFG-P) monitors the liquid level change in the tank at both stagnant and flow conditions. Global dynamic liquid hold-up was quantified volumetrically at different liquid loads by monitoring the level difference between stagnant and flow conditions and compensating for the liquid volumes present in the piping runs, pump, and liquid distributor. The indicator monitors levels of 0-300mm with an accuracy of 0.5mm (resolution of 0.1mm), therefore providing a global liquid hold-up measurement accuracy of approximately ±0.23%).

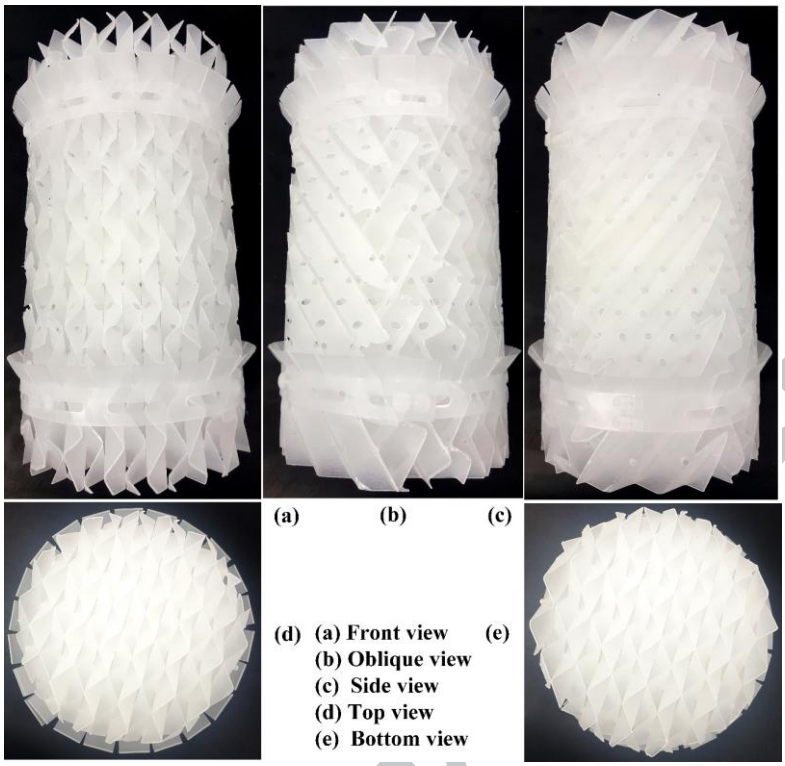

Fig.10. New Sulzer Mellapak 250Y structured packing

Fig. 10 shows the new polypropylene Sulzer Mellapak 250Y structured packing in the column. The relative permittivity of the packing material is about 2.2, which is the same value used in the simulation of section 3. The fraction of the packing material is 12% based on the manufacturer specifications.

The ECT sensor electrodes, described previously in Fig. 4, were positioned 350mm from the top of the column, effectively imaging the section 150 mm - 250 mm from the top of the packing. Previous work has demonstrated that increasing the of number of ECT electrodes does not increase tomogram image resolution [32], therefore 8 electrodes are used in this ECT sensor. An electrode height of 100 mm and a duty ratio of 0.88 were chosen based on previous studies of optimal ECT sensor design [33; 34]. Based on this electrode design, the spatial resolution of ECT has been estimated to be ~5% of column diameter, or ~9.5 mm [27].

ECT has typically been used in applications where the fluids being measured have very different electrical permittivities and are non-conductive. In gas-liquid mass transfer applications, the liquid and gas have different permittivities [35; 36], but the liquid tends to be electrically conductive and has a conductivity that can change over time. A typical example would be CO_2 scrubbing from a gas using an aqueous amine solvent, where the electrical conductivity of the solution can vary from 0 - 40mS/cm [37; 38] depending on the level of CO_2 absorbed. Previous work shows that liquid conductivity can have an impact on ECT measurement performance, but suggests that increasing the excitation frequency of the system can minimize the effect [39]. Additionally it was demonstrated that an imaged object which is electrically grounded becomes invisible to ECT [40], implying that a highly conductive liquid may need to be electrically floating to be able to be imaged by ECT. This effect likely occurs because when the liquid is connected to the ground, an electrical charge exchange happens between liquid phases that are inside and outside of the viewing field. The liquid can be seen as an equipotential body connected to the ground, and the calculated capacitance will be constant regardless of the amount of liquid present in the viewing field. In order to understand the effect of liquid phase electrical conductivity on the ECT measurement performance, two aqueous NaCl solutions with conductivities of 0.1mS/cm and 30mS/cm were used in this experiment.

The measurement procedure begins with an empty air-filled pipe ECT reference calibration measurement to determine C_{ref}. Next, the dry packing material is added into the column and a second ECT measurement is made to determine the fraction of

the packing. Finally, the NaCl solution is sprayed at the top of the column to conduct the experiment. Liquid load was varied from 13-39 m^3/m^2h and ECT measurements were used to compute the liquid hold-up at the cross section and to reconstruct the liquid distribution using the calculation method with common sensitivity matrix determined in section 3.2.

Global liquid hold-up was computed from liquid tank level difference using the level indicator and compared with the local hold-up measurements take from the ECT sensor.

5. Results and Discussions

5.1 Liquid Distribution

5.1.1 Tomographic cross section images: low conductivity

A NaCl solution with 0.1mS/cm electrical conductivity was used to represent a low conductivity liquid. 2D reconstructed tomogram images for a range of liquid loads are shown in Fig. 11, with the colored scale bar representing the normalized liquid distribution. The image is reconstructed from an average of 7140 frame taken over 10 seconds. A cutout 3D time series tomogram is also displayed in Fig. 11 to show the variation of the image over the 10 second measurement time.

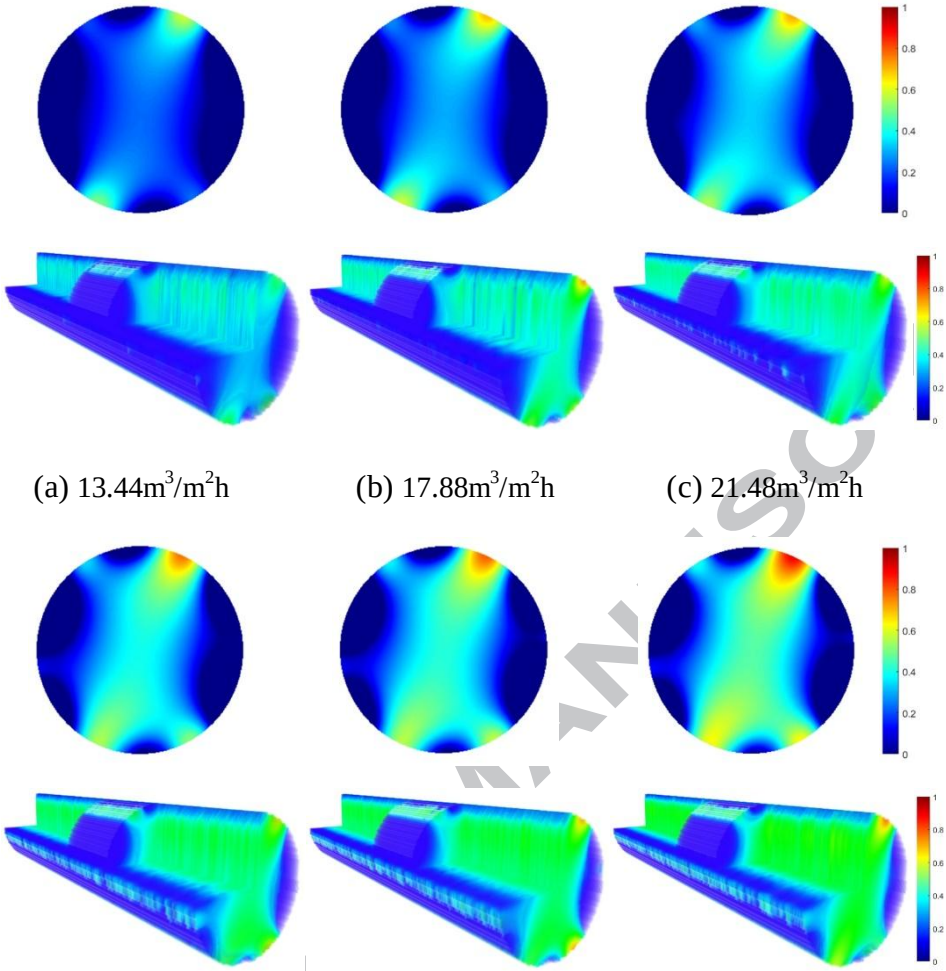

(a) 13.44m^3/m^2h (b) 17.88m^3/m^2h (c) 21.48m^3/m^2h

(d) 28.89m^3/m^2h (e) 31.70m^3/m^2h (f) 36.61m^3/m^2h

Fig.11. Reconstructed liquid distribution at different liquid load (0.1mS/cm)

The tomograms in Fig. 11 show not only the intuitive result that liquid hold-up on the packing increases with liquid load but also a banding like liquid distribution, with liquid forming predominantly in two channels at low liquid loads and starting to form in a third at higher liquid loads (Fig. 11 (d) - (f)). Additionally, liquid hold-up appears to pool at specific edges of the column with the pooling increasing as liquid load increases. This relatively poor liquid distribution is to be expected in the top most set of packing when liquid is distributed in a 60mm diameter in the center of the

packing. Liquid is directed into the packing channels at the center of the packing, travels predominantly along central channels to the column wall and is eventually redistributed via a packing wall wiper. A small portion of the liquid is able to transfer between packing sheet corrugations travelling along a second path before coming in to contact with the column wall. As liquid load increases, a meaningful portion of that diverted liquid is also able to transfer between sheets and travel along a third channel path. This banding liquid distribution behavior in the top most packing section has also been observed in Mellapak 250.X in literature [10](Figure 6 (a) - (d), point Z_2). The pooling at points on the column wall is observed because the relatively narrow column diameter (190mm vs 400mm), more gradual packing inclination angle (49° vs 30° from vertical), and wider viewing field (100mm vs ~<5mm) facilitate the liquid flowing toward the column wall within the viewing field in this work. In the previous study, the liquid reaches the column wall further down the packing and outside of the viewing field.

5.1.2 Tomographic cross section images: high conductivity

An NaCl solution with a 30 mS/cm electrical conductivity was used to represent a high conductivity liquid. 2D reconstructed tomogram images and cutout 3D time series tomograms are displayed in Fig. 12 in the same manner as described in section 5.1.1.

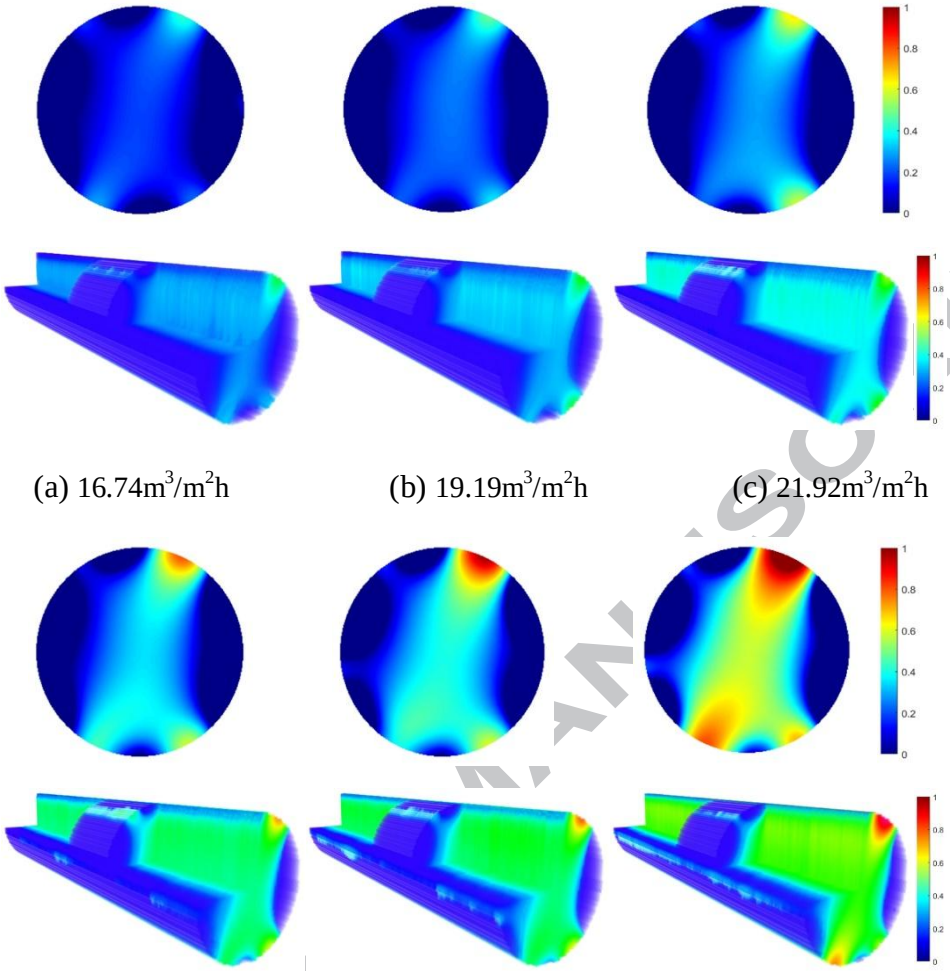

(a) 16.74m^3/m^2h (b) 19.19m^3/m^2h (c) 21.92m^3/m^2h

(d) 28.48 m^3/m^2h (e) 32.23 m^3/m^2h (f) 38.85 m^3/m^2h

Fig.12. Reconstructed liquid distribution with different liquid load (30mS/cm)

The tomograms in Fig. 12 show a liquid distribution behavior similar to that of the low conductivity test shown in Fig. 11, with liquid hold-up increasing with liquid load and liquid distribution predominately flowing in two distinct bands at low liquid loads before increasing to three bands at higher liquid loads.

Inspection of the packing section after testing (by dyed liquid) confirmed the banding flow pattern as mineral scaling visually observed in the small circular pattern of a diameter similar to the liquid distributor was observed at the top of the packing

(Fig. 13 (d)) spreading into a banding pattern along the length (Fig. 13 (a) - (c) and at the bottom of the packing section (Fig. 13 (e)).

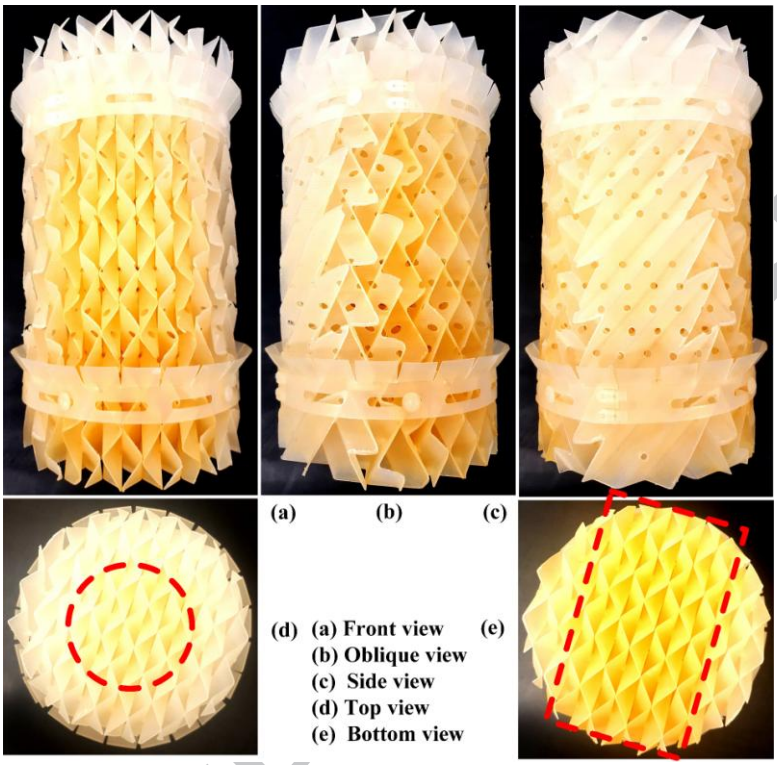

Fig.13. Used packing images caused by colored liquid

5.1.3 Impact of inclination angle on radial distribution of averaged liquid hold-up

Tomogram images can be deconstructed to provide a distribution of liquid hold-up on the packing averaged radially from the center of a column. Such distributions are useful for the characterization of packing hydrodynamics through empirical correlations, such as spread factor [41; 42]. Fourati reported distributions of liquid hold-up averaged radially for a 400 mm diameter column filled with 1.5m of stainless steel Mellapak 250.X structured packing using high resolution gamma-ray tomography [10]. Fig. 14 shows a comparison of the normalized liquid hold-up

distribution of stainless steel Mellapak 250.X imaged with gamma-ray tomography at a depth of 190 mm down the first packing section in Fourati' work and the normalized liquid hold-up distribution of Mellapak 250.Y PP imaged with ECT tomography over a depth of 150-250 mm down the first packing section in this work.

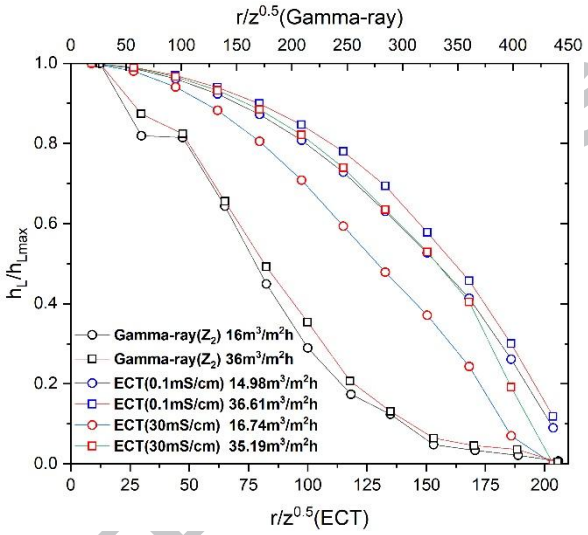

Fig.14. Averaged radial distribution of local liquid hold-up measured with ECT and high resolution gamma-ray tomography [10].

The x-axis of Fig. 14 has been scaled to account for the difference in column diameter between the experiments with the larger gamma ray column study displayed on the top and the smaller ECT column study displayed on the bottom. The settings of the figure are the same with Fourati, where h_L and h_{Lmax} are the liquid hold-up and the maximum liquid hold-up value in the current liquid load separately, z and r indicate respectively, the axial and the radial positions in acylindrical coordinates system. Fig. 14 demonstrates first that the averaged radial distribution of liquid hold-up appears to maintain the same shape perhaps with a slight broadening as liquid load increases, as

can be observed by comparing the gamma-ray, ECT low conductivity and ECT high conductivity data pairs at 16 and 36 m^3/m^2h. Fig. 14 also shows the impact of inclination angle on liquid spreading behavior and distribution through structured packing. In both experiments, liquid is injected into the center of a set of packing and the packing geometry (corrugation angle, sheet perforation hole size and density, channel size) is similar with the exception sheet material, sheet geometry, and inclination angle. Stainless steel Mellapak 250.X has a steep inclination angle of 30° from vertical and as such its radial liquid hold-up distribution profile is fairly narrow at the packing depth of 190mm. The liquid is spreading out radially across this packing from the center packing channels, but the spreading has not completely reached the column wall.

In contrast, Mellapak 250.Y PP has a much more gradual inclination angle of 49° from vertical and as such has a much broader radial liquid hold-up distribution profile. Liquid is able to spread from the center packing channels more rapidly achieving a broader liquid distribution across the first packing section more rapidly than Mellapak 250.X. This data can meet the knowledge that a steeper inclination angle allows for a higher liquid load to be used and has lower pressure drop but requires a little bit higher packing height to get everything distributed.

5.2 Real-Time Measurement of Liquid Hold-up

Previously, a major drawback of radiation based (x-ray and gamma-ray) tomography techniques is that images are acquired at rates that are too slow to

observe liquid hydrodynamics on packing structures. Recent advances have introduced an ultra-fast electron beam x-ray tomography technology that is capable of drastically improving the image acquisition rate on relatively narrow columns of 80mm diameter [43] at acquisition rates of 2000 frames per second with a measurement resolution of ~1mm (~1.25% of column diameter). Janzen [11] used the ultra-fast tomography system to provide new insights into temporal evolution of liquid hold-up for an 80mm diameter column packed with stainless steel Montz B1-350 MN and B1-500 MN structured packings at various depths down the first and second packing elements. Fig. 15 shows a comparison of temporal evolution of liquid hold-up deconstructed from ultra-fast electron beam x-ray tomograms for Montz B1-350 MN and B1-500 MN at F-factors below the flooding point with liquid hold-up data reported from deconstructions of ECT tomograms of Mellapak 250.Y PP in this work.

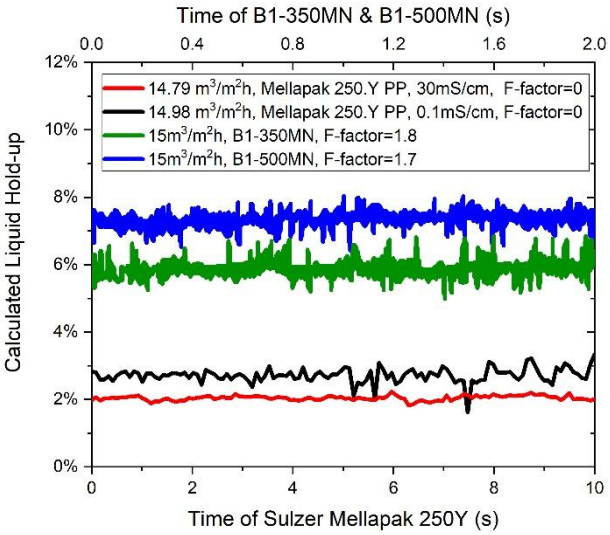

Fig.15. Temporal evolution of local liquid hold-up measured by ECT tomography and ultra-fast electron beam tomography [11]

The x-axis of Fig. 15 has been scaled to account for the difference in acquisition time between the experiments with the x-ray study acquiring over two seconds displayed on the top and ECT study acquiring over ten seconds displayed on the bottom. The x-ray study acquires data significantly faster than the ECT used in this work (2000 fps vs 714 fps), has a significantly higher measurement resolution (1.25% vs 5% of column diameter) and is measuring over a smaller column diameter (80mm vs 190mm), but analyzed liquid distribution and hold-up at similar depths down the first set of packing. A comparison of the results in Fig. 15 demonstrates first the intuitive observation that the liquid hold-up values are highly dependent on the surface area of the structured packing material, with Mellapak 250.Y PP (250 m^2/m^3) having a lowest liquid hold-up, Montz B1-350MN ($350m^2/m^3$) having a higher liquid hold-up value and Montz B1-500MN (500 m^2/m^3) having the highest liquid hold-up.

Janzen made the observation that below packing flooding points liquid hold-up appears to stay constant fluctuating ~0.5% around the mean value, which would validate the commonly held assumption that steady liquid flows and spatial liquid flow distributions exist below the flooding point. The comparison in Fig. 15 provides further evidence for that observation with liquid hold-up for Mellapak 250.Y PP also remaining constant and fluctuating ~0.5% around the mean value. It is interesting to note that this work appears to show these temporal liquid hold-up fluctuations are present even in a no gas flow condition.

5.3 Overall Liquid Hold-up

Local liquid hold-up values are computed from the deconstructed ECT tomograms, providing insight into the packing wettability and allow for comparison with global liquid hold-up values both measured experimentally and taken from empirical correlations. Fig. 16 compares the local liquid hold-up values computed from the ECT tomograms measured 150-250mm deep into the first Mellapak 250.Y PP packing element compared to global liquid hold-up values, both measured volumetrically by tank level as described in section 4 and from Mellapak 250.Y correlations available in literature [2; 4; 44].

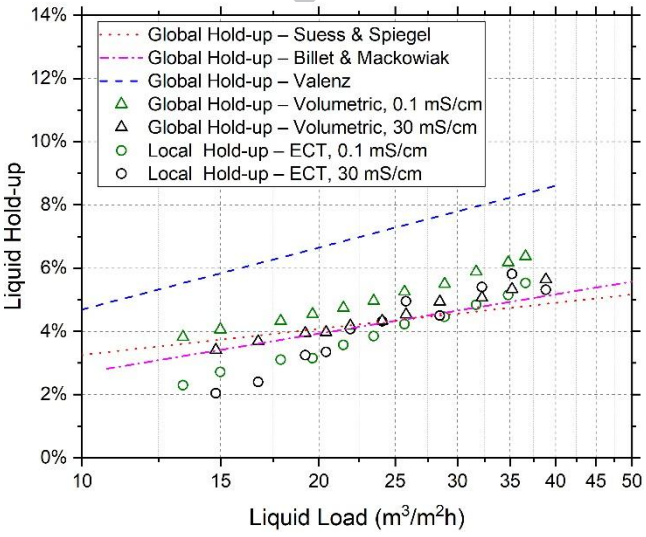

Fig. 16. Hold-up versus liquid load measured locally by ECT tomography and globally by tank level differential. Literature correlations from Suess & Spiegel [4], Billet & Macowiak [2] and Valenz et al. [44].

The empirical correlations shown in Fig. 16 were all derived from experimental

data on counter-current gas liquid columns packed with stainless steel Mellapak 250.Y structured packing. Billet & Mackowiak measured the global liquid hold-up volumetrically with a drain and collect procedure on a column with a diameter of 220mm, a packing height of 1.4m and no gas flow. Valenz measured the global liquid hold-up by conductive probe installed in each of the four liquid outlet tubes of the column to monitor the concentration of the liquid tracer. The column has a diameter of 297mm, a packing height of 0.84m and no gas flow in this condition. Suess and Spiegel measured the global liquid hold-up with a gamma-ray densitometer on a column with a diameter of 1000mm, a packing height of 3.5m and a low gas F-factor of 0.5 m/s $(kg/m^3)^{0.5}$.

The comparisons in Fig. 16 show first that the tank level differential volumetric global hold-up measurement technique proposed in section 4 appears to closely match the empirical global liquid hold-up correlations, particularly those of Suess & Spiegel and Billet & Macowiak. Although it should be noted that Mellapak 250.Y PP has an inclination angle of 49° from vertical compared with 45° from vertical for stainless steel Mellapak 250.Y. Additionally, while the corrugation angle and sheet perforation density and hole sizes are similar, the sheet geometry is different with stainless steel Mellapak 250.Y having a more undulating surface while 250.Y PP is largely a flat plastic sheet. These differences may explain the slight deviation from the available correlations. The global hold-up measurement data presented here seems to follow the 0.66 power law observed in Billet and Valenz as opposed to the 0.59 power law proposed in Suess. It is also interesting to note that the global liquid hold-up values

for the low conductivity liquid are larger overall than the high conductivity liquid at equivalent liquid loads. This observation may confirm the commonly held assumption that liquid surface tension has an impact on liquid film thickness and therefore global liquid hold-up because the NaCl solution with higher conductivity and lower surface tension has a lower global liquid hold-up.

Fig. 16 also shows that the local liquid hold-up computed from deconstructed ECT tomograms also follows the correlations fairly well. Tomograms displayed in Fig. 11 and Fig. 12 show that the liquid in this region of the first set of packing has not yet achieved optimum distribution, predominately flowing to 2-3 channel directions. Therefore, it is likely the liquid hold-up behavior may not precisely follow the global hold-up values nor the power law behavior of the global liquid hold-up correlations. This appears to be the case for both the low and high conductivity local hold-up datasets, under-estimating the global hold-up correlations in the 13 - 25 m^3/m^2h liquid loading range and then over-estimating the correlations in the 35 - 45 m^3/m^2h range.

The high and low conductivity datasets appear to both follow the same linear pattern but with the high conductivity dataset providing a larger degree of variance in the readings. A possible explanation for this variance is that high conductivity media, particularly liquid droplets located near the pipe wall, may be causing imaging artifacts that disturb the electrical permittivity measurements in the viewing field. This effect might be mitigated in applications where gas flow and packing internals such as wipers minimize the formation of droplets on the column wall. Another possible explanation for this variance would be the effect of electromagnetic

interference from other equipment such as the liquid pump and flow sensors. Complete electromagnetic shielding of the viewing field might mitigate this effect. Finally, another explanation of the variance could be the ability of the liquid phase in the viewing field to find electrical ground or some other form of leakage current, which could also cause imaging artifacts. This affect is unlikely considering the non-continuous nature of the liquid phase on the packing with other grounded liquid phases, for example in tanks and pipe runs, but may be mitigated through empirical correction factors.

6. Conclusions

A method was proposed for calculating the liquid phase distribution in a gas-liquid packed column in industrial field applications, such as amine based post combustion CO_2 capture. The proposed method utilizes electrical capacitance tomography (ECT) measurements that can be made with low-cost probes capable of being installed external to packed columns and operated in a convenient and safe manner, however the method would not be effective when imaging metallic packings that would facilitate charge transfer from the liquid phase. The proposed method also makes strategic simplifications to the traditional ECT calibration and measurement procedure in order to perform the liquid phase calculation in a way that is convenient for industrial field use. These include eliminating the requirement of a fully flooded viewing field reference measurement and the requirement of calibration and normalization of electrical field measurements against local liquid hold-up

measurements prior to operation. The alternative only requires vacant and dry calibration steps.

The validity of these strategic simplifications were confirmed through finite element analysis (FEM) studies. These studies confirmed first that neither packing geometry nor packing orientation relative to the tomography probe had a significant impact on phase identification and second that liquid has different permittivities can be measured by the model based on the revision of the coefficient. FEM analysis was then used to demonstrate the theoretical accuracy of the proposed calculation method in a typical gas-liquid absorption application using complex packing structure, constructed from polypropylene.

An experimental campaign was performed using a 190mm diameter packed column fitted with 4 sections of Mellapak 250.Y PP totaling 945mm in height. The tomography sensor, positioned to image the depth of 150 - 250mm down the first set of packing, effective showed that the liquid distribution had yet to fully wet the packing instead flowing predominantly through 2 - 3 channel paths. Comparison of the radial averaged liquid distribution with a gamma-ray tomography study on Mellapak 250.X shows that the inclination angle of structured packing corrugation sheets has an impact on the radial distribution of liquid hold-up in the upper portions of packed beds. Comparison of the temporal evolution of liquid hold-up with an ultra-fast x-ray tomography study of Montz B1-350 MN and B1-500 MN shows that liquid hold-up fluctuations of ~0.5% are observable below the flooding limit and even at no gas flow conditions. Analysis of local liquid hold-up values in the viewing field

shows reasonable agreement with both global liquid hold-up values measured experimentally and with empirical correlations from literature.

Data from low and high conductivity liquids suggest the proposed method is capable of analyzing aqueous absorption solvents, but higher measurement noise and variance was observed in the high conductivity test. Potential reasons for the variance include high conductivity droplets on the column wall causing measurement artifacts, electromagnetic interference from other equipment, and charge transfer or electrical earthing of the liquid in the viewing field. Overall the experimental campaign was able to provide confidence that proposed calculation method could be suitable for industrial field service in gas-liquid packed columns and demonstrate that an ECT system is able to provide in-situ liquid distribution measurements which could be used for accurate real-time liquid distribution and local liquid hold-up measurements.

Acknowledgment

The authors would like to express their gratitude for the support from the UK Engineering and Physical Sciences Research Council (EPSRC, EP/M001482/1), The National Natural Science Foundation of China-the Royal Society of Edinburgh (NSFC-RSE, No. 6151101270) and China Scholarship Council (CSC). Dr. Mathieu Lucquiaud was financially supported by a UK Royal Academy of Engineering Research Fellowship during this research.

References

[1] K.J. Mcnulty, and C. Hsieh, Hydraulic performance and efficiency of koch flexipac structured packings, AIChE Annu. Meeting, 1982.

[2] R. Billet, and J. Mackowiak, Application of modern packings in thermal separation processes. Chem. Eng. Technol. (1988) 213-227.

[3] J. Maćkowiak, Fluiddynamik von kolonnen mit modernen füllkörpern und packungen für gas-flüssigkeitssysteme, Salle, (1991).

[4] P. Suess, and L. Spiegel, Hold-up of mellapak structured packings. Chemical Engineering and Processing: Process. Intensification 31 (1992) 119-124.

[5] E. Brunazzi, A. Paglianti, L. Spiegel, and F. Tolaini, Hydrodynamics of a gas-liquid column equipped with mellapakplus packing, Proceedings of the Seventh International Conference on Distillation and Absorption, Baden-Baden, DE, 2002, pp. 1-18.

[6] K. Salem, E. Tsotsas, and D. Mewes, Tomographic measurement of breakthrough in a packed bed adsorber. Chem. Eng. Sci. 60 (2005) 517-522.

[7] D. Toye, P. Marchot, M. Crine, and G. L'Homme, Modelling of multiphase flow in packed beds by computer-assisted x-ray tomography. Measurement Science & Technology 7 (1996) 436-443.

[8] D. Toye, M. Crine, and P. Marchot, Imaging of liquid distribution in reactive distillation packings with a new high-energy x-ray tomograph. Meas. Sci. Technol. 16 (2005) 2213-2220.

[9] M. Schubert, G. Hessel, C. Zippe, R. Lange, and U. Hampel, Liquid flow texture analysis in trickle bed reactors using high-resolution gamma ray tomography. Chem. Eng. J. 140 (2008) 332-340.

[10] M. Fourati, V. Roig, and L. Raynal, Experimental study of liquid spreading in structured packings.

Chem. Eng. Sci. 80 (2012) 1-15.

[11] A. Janzen, M. Schubert, F. Barthel, U. Hampel, and E.Y. Kenig, Investigation of dynamic liquid distribution and hold-up in structured packings using ultrafast electron beam x-ray tomography. Chemical Engineering and Processing: Process. Intensification 66 (2013) 20-26.

[12] A. Janzen, J. Steube, S. Aferka, E.Y. Kenig, M. Crine, P. Marchot, and D. Toye, Investigation of liquid flow morphology inside a structured packing using x-ray tomography. Chem. Eng. Sci. 102 (2013) 451-460.

[13] M. Bieberle, and F. Barthel, Combined phase distribution and particle velocity measurement in spout fluidized beds by ultrafast x-ray computed tomography. Chem. Eng. J. 285 (2016) 218-227.

[14] A. Aroonwilas, A. Chakma, P. Tontiwachwuthikul, and A. Veawab, Mathematical modelling of mass-transfer and hydrodynamics in co2 absorbers packed with structured packings. Chem. Eng. Sci. 58 (2003) 4037-4053.

[15] C. Soulaine, P. Horgue, J. Franc, and M. Quintard, Gas-liquid flow modeling in columns equipped with structured packing. Aiche J. 60 (2014) 3665-3674.

[16] Y. Haroun, L. Raynal, and D. Legendre, Mass transfer and liquid hold-up determination in structured packing by cfd. Chem. Eng. Sci. 75 (2012) 342-348.

[17] E. Brunazzi, A. Paglianti, and S. Pintus, A capacitance probe and a new model to identify and predict the capacity of columns equipped with structured packings. Ind. Eng. Chem. Res. 40 (2001) 1205-1212.

[18] A. Muzen, and M.C. Cassanello, Liquid holdup in columns packed with structured packings: countercurrent vs cocurrent operation. Chem. Eng. Sci. 60 (2005) 6226-6234.

[19] M. Hamood-Ur-Rehman, Y. Dahman, and F. Ein-Mozaffari, Investigation of mixing

characteristics in a packed-bed external loop airlift bioreactor using tomography images. Chem. Eng. J. 213 (2012) 50-61.

[20] T. Eda, A. Sapkota, J. Haruta, M. Nishio, and M. Takei, Experimental study on liquid spread and maldistribution in the trickle bed reactor using electrical resistance tomography. Journal of Power and Energy Systems 7 (2013) 94-105.

[21] H. Wang, J. Jia, B. Buschle, and M. Lucquiaud, Effect of packing and liquid conductivity on gas distribution and holdup in reaction column, IEEE International Instrumentation and Measurement Technology Conference Proceedings, 2016, pp. 1-6.

[22] Y. Son, G. Kim, S. Lee, H. Kim, K. Min, and K.S. Lee, Experimental investigation of liquid distribution in a packed column with structured packing under permanent tilt and roll motions using electrical resistance tomography. Chem. Eng. Sci. 166 (2017) 168-180.

[23] N. Reinecke, and D. Mewes, Investigation of the two phase flow in trickle-bed reactors using capacitance tomography. Chem. Eng. Sci. 52 (1997) 2111-2127.

[24] R.B. White, Using electrical capacitance tomography to monitor gas voids in a packed bed of solids. Meas. Sci. Technol. 13 (2002) 1842-1847.

[25] M. Hamidipour, and F. Larachi, Characterizing the liquid dynamics in cocurrent gas-liquid flows in porous media using twin-plane electrical capacitance tomography. Chem. Eng. J. 165 (2010) 310-323.

[26] W. Yang, and L. Peng, Image reconstruction algorithms for electrical capacitance tomography. Meas. Sci. Technol. 14 (2003) R1.

[27] L. Jérôme, and C. Margo, Physical limitations on spatial resolution in electrical capacitance tomography. Meas. Sci. Technol. 26 (2015) 125105.

[28] Y. Yang, and L. Peng, A configurable electrical capacitance tomography system using a combining electrode strategy. Meas. Sci. Technol. 24 (2013).

[29] Y. Yang, L. Peng, and J. Jia, A novel multi-electrode sensing strategy for electrical capacitance tomography with ultra-low dynamic range. Flow Meas. Instrum. 53 (2017) 67-79.

[30] T.R. Mckeen, and T.S. Pugsley, The influence of permittivity models on phantom images obtained from electrical capacitance tomography. Meas. Sci. Technol. 13 (2002) 1822.

[31] Y. Li, W. Yang, C. Xie, S. Huang, Z. Wu, D. Tsamakis, and C. Lenn, Gas/oil/water flow measurement by electrical capacitance tomography. Meas. Sci. Technol. 24 (2013) 74001.

[32] L. Peng, J. Ye, G. Lu, and W. Yang, Evaluation of effect of number of electrodes in ECT sensors on image quality. IEEE Sens. J. 12 (2012) 1554-1565.

[33] L.H. Peng, C.H. Mou, D.Y. Yao, B.F. Zhang, and D.Y. Xiao, Determination of the optimal axial length of the electrode in an electrical capacitance tomography sensor. Flow Meas. Instrum. 16 (2005) 169-175.

[34] W. Yang, Design of electrical capacitance tomography sensors. Meas. Sci. Technol. 21 (2010) 42001.

[35] X. Li, Z. Huang, B. Wang, and H. Li, A new method for the online voidage measurement of the gas-oil two-phase flow. IEEE Transactions onInstrumentation and Measurement 58 (2009) 1571-1577.

[36] C. Rautenbach, M.C. Melaaen, and B.M. Halvorsen, Statistical diagnosis of a gas-solid fluidized bed using electrical capacitance tomography. Int. J. Multiphas. Flow 49 (2013) 70-77.

[37] S. Han, and J. Wee, Estimation of correlation between electrical conductivity and co2 absorption in a monoethanolamine solvent system. Journal of Chemical & Engineering Data 58 (2013)

2381-2388.

[38] S. Han, and J. Wee, Estimation of the amount of co2 absorbed by measuring the variation of electrical conductivity in highly concentrated monoethanolamine solvent systems. Journal of Chemical & Engineering Data 61 (2016) 712-720.

[39] Y. Li, and M. Soleimani, Imaging conductive materials with high frequency electrical capacitance tomography. Measurement 46 (2013) 3355-3361.

[40] M. Zhang, and M. Soleimani, Imaging floating metals and dielectric objects using electrical capacitance tomography. Measurement 74 (2015) 143-149.

[41] K. Porter, and M. Jones, A theoretical prediction of liquid distribution in a packed column with wall effect. Trans. Inst. Chem. Eng. 41 (1963).

[42] K. Onda, H. Takeuchi, Y. Maeda, and N. Takeuchi, Liquid distribution in a packed column. Chem. Eng. Sci. 28 (1973) 1677-1683.

[43] F. Fischer, D. Hoppe, E. Schleicher, G. Mattausch, H. Flaske, R. Bartel, and U. Hampel, An ultra fast electron beam x-ray tomography scanner. Meas. Sci. Technol. 19 (2008) 94002.

[44] L. Valenz, F.J. Rejl, and V. Linek, Gas and liquid axial mixing in the column packed with mellapak 250y, pall rings 25, and intalox saddles 25 under flow conditions prevailing in distillation columns. Ind. Eng. Chem. Res. 49 (2010) 10016-10025.

Highlights

- Simplified electrical capacitance tomography (ECT) model and calibration method are developed.
- The accuracy of the proposed measurement procedure is validated in the FEM models.
- Liquid distribution and hold-up in packed column are measured by ECT are compared with other previous studies.
- The inclination angle of structured packing corrugation sheets has a great impact on the radial distribution of liquid hold-up.